Bioengineering

AIMS Bioengineering, 13(2): 281–294.
DOI: 10.3934/bioeng.2026013
Received: 07 May 2026
Revised: 07 June 2026
Accepted: 12 June 2026
Published: 25 June 2026

https://www.aimspress.com/journal/Bioengineering

Research article

Utilization of an 810 nm diode laser for the eradication of *Staphylococcus aureus* on implant surfaces: an in vitro study

Thuy Vo*, Loan Pham, Luong Dau, Tien Ho, Duc Cao and Lam Bui

Department of Dental Implantology, Faculty of Dentistry, University of Medicine and Pharmacy at Ho Chi Minh city, Vietnam

* **Correspondence:** Email: thuyvo@ump.edu.vn.

Abstract: Peri-implantitis is a prevalent complication in dental implantology, often resulting from bacterial contamination on implant surfaces. Researchers have explored diode lasers as a promising alternative for bacterial decontamination. In this study, we evaluated the effectiveness of the 810 nm diode laser in eliminating *Staphylococcus aureus* from titanium implant surfaces. This investigation was designed as a controlled, standardized in vitro laboratory experiment. A total of 95 titanium implants were divided into the following groups: (1) A negative control group (n = 5): New integrity implants; (2) a positive control group (n = 6): Implants contaminated with a *S. aureus* suspension and left untreated; and (3) four intervention groups (n = 21 for each group): Implants contaminated and then treated with the 810 nm diode laser at varying power settings (1 W, 1.5 W, 2 W, 2.5 W) for 3 minutes. Bacterial load was quantified using colony-forming unit analysis, while surface roughness and morphology were assessed with a surface roughness tester and scanning electron microscopy (SEM) after laser treatment. The results showed that all intervention groups demonstrated significant reductions in bacterial load compared to the positive control group, with bacterial reduction increasing with higher laser power. The 2.5 W settings proved most effective in decontamination, although none of the laser settings completely eradicated the bacteria. Laser treatment did not result in significant changes in implant surface roughness, suggesting its safety for use in surface decontamination without compromising implant integrity. This technology may represent a safer, more effective approach to implant surface decontamination than traditional methods.

Keywords: 810 nm diode laser; *Staphylococcus aureus;* titanium implants; dental implant surface; laser eradication; in vitro study

1. Introduction

Dental implants have become popular for replacing missing teeth due to their high success rates and ability to restore function and aesthetics [1]. Despite the advantages, peri-implantitis remains a significant complication following dental implant procedures [2]. Peri-implantitis is an inflammatory condition that affects the soft and hard tissues surrounding an implant, leading to progressive bone loss and, in severe cases, implant failure [3]. The condition is primarily caused by bacterial infections that lead to the formation of biofilms on the implant surface, making effective treatment challenging [4].

Among the bacterial species involved in peri-implantitis, *Staphylococcus aureus* is one of the most commonly isolated pathogens [5,6]. This pathogen is notorious for its ability to form biofilms, which are clusters of bacterial cells embedded in a protective matrix. Biofilm formation significantly complicates the treatment of peri-implant infections, as biofilms protect bacteria from the host immune system and antimicrobial therapies [7,8]. In peri-implantitis, *S. aureus* adheres to the titanium surface of the implant, where it can thrive, evade antibiotic treatment, and induce inflammation.

Traditional methods for managing peri-implantitis involve mechanical debridement, chemical antiseptics, and, in more severe cases, surgical intervention. Mechanical cleaning methods, such as ultrasonic scalers and curettes, are commonly used to remove plaque and calculus from the implant surface. However, these techniques often fail to adequately address the bacterial biofilm, particularly on roughened titanium surfaces, and they may cause damage to the implant, reducing its long-term success [9,10]. Similarly, chemical treatments like chlorhexidine or hydrogen peroxide have shown varying degrees of success, but they are also limited by issues such as potential toxicity and residual chemical effects, which can impair osseointegration [11,12].

To address these limitations, there has been growing interest in laser-based therapies as an alternative or adjunctive method for treating peri-implantitis [13–18]. Lasers offer the potential to target bacterial cells selectively while minimizing damage to surrounding tissues and the implant surface. Among laser types, diode lasers, particularly those operating at a wavelength of 810 nm, have been studied extensively for their ability to provide precise bacterial decontamination [19,20]. The 810 nm wavelength lies within the near-infrared spectrum, where it is efficiently absorbed by water and other chromophores in bacterial cells, leading to a photothermal effect that causes bacterial cell death [21,22].

One of the major advantages of using diode lasers for peri-implantitis treatment is their selective action. Diode lasers are known to target the bacterial biofilm with minimal effect on the surrounding tissues and the titanium implant surface, which is crucial for maintaining osseointegration [13]. Additionally, diode lasers can penetrate the biofilm and eliminate bacteria from areas that are difficult to reach with traditional mechanical or chemical methods [14]. Several researchers have reported significant reductions in bacterial load following laser treatment, with minimal changes in the implant surface roughness, which is essential for the success of osseointegration [22–24].

Despite these promising results, there are concerns regarding the optimal settings for laser treatment, such as the appropriate power level and duration of exposure. Higher power settings may improve bacterial eradication but could potentially lead to alterations in the surface properties of the implant, such as changes in roughness or surface morphology [25,26]. These changes may, in turn, affect the ability of the implant to integrate with the bone. Therefore, it is essential to balance effective bacterial decontamination with the preservation of implant surface integrity to ensure long-term implant success. In addition, in vitro studies have demonstrated that diode lasers can achieve bacterial reduction rates exceeding 99%; many of these investigations were conducted using flat titanium discs [27,28]. Such

models do not accurately simulate the "shadow zones" and complex geometric challenges presented by actual threaded dental implants.

Our primary aim of this study was to investigate the efficacy of the 810 nm diode laser in eradicating *S. aureus* from titanium implant surfaces under different laser power settings. We also aimed to assess the impact of laser treatment on the surface roughness and morphology of the implants. By addressing these key factors, we seek to contribute to the growing body of evidence supporting the use of diode lasers in peri-implantitis treatment and to provide guidelines for their optimal use in clinical practice.

2. **Materials and methods**

2.1. Study design

This study was designed as a controlled in vitro experiment to evaluate the effectiveness of the 810 nm diode laser in decontaminating titanium implant surfaces infected with *S. aureus*. Because this protocol was conducted strictly within a controlled laboratory environment, clinical trial design classifications (such as prospective, retrospective, randomized controlled, split-mouth, or patient observational frameworks) were not applicable. The implants used in the study were real titanium dental implants (Biotem, Korea), size 3.5 × 10 mm, treated with sandblasting and acid etching (SLA treatment). A total of 95 titanium implants were divided into the following groups: (1) A negative control group (n = 5): new intact implants; (2) a positive control group (n = 6): Implants contaminated with a *S. aureus* suspension and left untreated; and (3) four intervention groups (n = 21 for each group): Implants contaminated and then treated with the 810 nm diode laser at varying power settings (1 W, 1.5 W, 2 W, 2.5 W) for 3 minutes. To isolate the absolute biophysical and photothermal decontamination capacity of the 810 nm wavelength and prevent confounding experimental variables, the laser was evaluated strictly as a standalone intervention within this laboratory model.

Bacterial decontamination, changes in implant surface roughness and morphological alterations were assessed post-treatment. The negative control group was utilized to define the unaltered baseline for surface roughness and micro-morphology, while the positive control group was utilized to quantify the native biofilm adherence and establish the biological baseline necessary to determine absolute post-treatment bacterial reduction percentages.

2.2. Bacterial strain and culture

The bacterial model used in this study was *S. aureus* strain ATCC 25923. The strain was activated by inoculating 1–2 colonies into Brain-Heart Infusion (BHI) broth and incubating the mixture at 37 °C for 6 hours. The resulting suspension was adjusted to a turbidity of 1×10^8 CFU/ml using a densitometer. To establish a biofilm on the titanium surfaces, each implant was submerged in 1 ml of the bacterial suspension and incubated in a 5% CO_2 environment at 37 °C for 72 hours. Before the laser intervention, all implants were rinsed three times with sterile phosphate-buffered saline (PBS) to remove any non-adherent bacteria.

2.3. Custom holder for laser treatment

We utilized a custom-designed mechanical fixation system to eliminate human error associated with manual handling and to maintain a constant distance between the laser tip and the titanium surface (Figure 1). The apparatus consisted of two major components:

- Implant Fixation Stand: Each implant was secured into a low-speed dental handpiece, which was then mounted onto a vertical stand. This configuration ensured that the longitudinal axis of the implant remained perfectly perpendicular to the floor throughout the procedure.
- Laser Handpiece Holder: The laser handpiece was secured in a secondary adjustable stand positioned opposite the implant. The holder was calibrated so that the laser tip (400 μm diameter) remained perpendicular to the implant's surface. The distance between the laser tip and the implant was adjusted so that the resulting laser spot covered the width of the implant (approximately 3.3–3.5 mm in diameter).

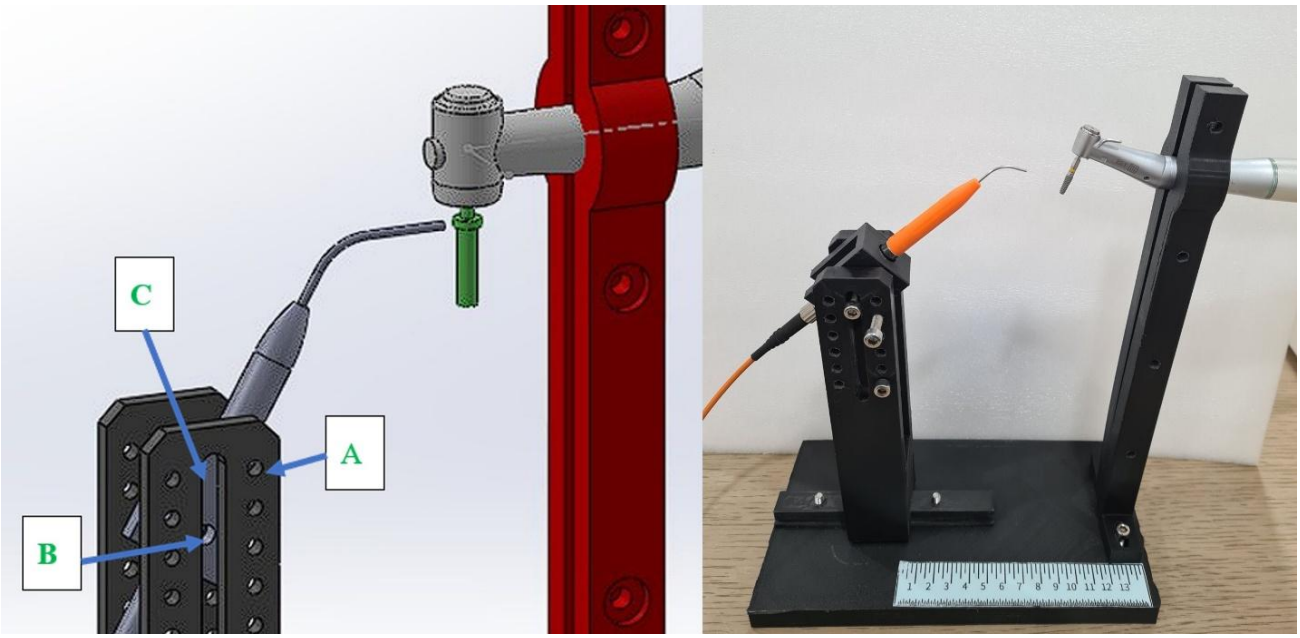

Figure 1. Customized holder for controlled laser decontamination of dental implants in schematic design (left) and actual experimental configuration (right). The system integrates three components: (A) Vertical pins for incremental height adjustment, (B) alignment pin, and (C) sliding track for parallel movement along the implant axis.

2.4. Laser treatment

The treatment was performed using the AMD LASER Picasso Lite Plus (AMD Lasers, USA), a GaAlAs diode laser system with a wavelength of 810 nm. To ensure maximum reproducibility, all fundamental biophysical parameters were standardized as follows:

* **Irradiation Mode:** Continuous-wave (CW) mode.
* **Power Settings:** Fully calibrated outputs of 1 W, 1.5 W, 2 W, and 2.5 W.
* **Fiber-Tip Specification:** Single-use quartz optical fiber tip with a diameter of 400 μm.

* **Application Distance and Spot Size:** Maintained at a fixed parallel distance via a custom mechanical holder, calibrating the beam divergence to produce a spot size covering the full implant diameter (3.3–3.5 mm).

* **Orientation:** Positioned at a constant, perpendicular angle relative to the implant's longitudinal axis.

* **Exposure Duration and Frequency:** A single, standardized intervention session lasting 3 minutes total per implant, vertically partitioned into three equal segments (neck, body, apex) irradiated for exactly 1 minute each.

* **Cooling Method:** Executed under dry ambient laboratory conditions without active coolant or irrigation, establishing an absolute thermal load ceiling.

During the irradiation process, the surgical motor (Surgery X) rotated the implant at a constant speed of 20 rpm. This rotation, combined with the fixed laser spot, ensured that the laser energy was distributed evenly across the circumference and into the depths of the implant threads. The procedure was conducted within a class II biological safety cabinet to maintain sterile conditions and prevent external contamination. All fiber-optic tips used were single-use to ensure consistency across samples.

2.5. Bacterial quantification

Immediately following the laser decontamination procedure, each implant was submerged in 1 ml of BHI broth and vortexed at maximum intensity for 1 minute to effectively detach residual bacteria from the titanium surface. A serial 10-fold dilution process was performed for each sample, extending up to seven consecutive dilutions. Aliquots of 100 μL from the diluted suspensions were then plated onto BHI agar (distributed across two plates at 50 μL each) and incubated under microaerophilic conditions for 48 hours. Colony-forming units (CFUs) were subsequently counted by an independent examiner, selecting plates with fewer than 200 colonies to ensure accuracy. The bacterial load reduction for each treatment group was calculated by comparing the CFU counts to those of the positive control group.

2.6. Scanning electron microscopy (SEM) examination

For qualitative analysis of the surface morphology, one random implant was selected from the positive control group and each of the four intervention groups. The selected samples were cleaned through a serial ethanol dehydration protocol (concentrations of 50%, 70%, 90%, and 99% for 15 minutes each) and dried. Surface examination was conducted using a Tescan Mira 4 scanning electron microscope. A technician, blinded to the experimental groups, randomly selected one thread on each implant to capture high-resolution images at four specific locations relative to the thread geometry. Observations were recorded at multiple magnifications, specifically X25, X50, X500, X1000, and X5000, to identify structural changes such as melting, debris, or loss of the characteristic vi-porous SLA structure.

2.7. Surface roughness assessment

Quantitative topographic changes were assessed using the implants from the negative control group and the remaining implants from the positive control and each intervention group (excluding

samples utilized for SEM). Following the serial ethanol cleaning and drying process, each implant was vertically partitioned into three distinct sections: the neck, body, and apex. Within each section, one thread was randomly selected for measurement at four locations; the top, middle, and bottom of the thread, and the trough, totaling 12 measurement points per implant. The average surface roughness (Ra), defined as the arithmetic mean of surface height deviations, was recorded using a specialized profilometer and its integrated software. The final group roughness value was calculated as the mean of all measured positions within that group.

2.8. Statistical analysis

All experimental data were statistically analyzed using SPSS software, version 22.0. The primary outcome measure was defined microbiologically as the quantitative reduction of bacterial concentration, evaluated via colony-forming unit counts (CFU/mL). The secondary outcome measures were defined topographically as the quantitative changes in Ra via profilometry, alongside qualitative changes in micro-morphology tracked via high-resolution SEM imaging.

Preliminary normality checking via the Shapiro-Wilk and Kolmogorov-Smirnov tests confirmed that the major variables across the experimental groups followed a non-normal distribution, justifying a non-parametric analytical framework. Because this study was strictly an in vitro laboratory experiment entailing manufactured implants, there were no human patients or multi-implant patient clustering errors to account for.

The Kruskal-Wallis test was used to assess significant differences in bacterial counts and Ra values across experimental groups and control groups. For subsequent pairwise comparisons between any two specific groups, the Mann-Whitney U test was performed. All statistical tests were conducted with a 95% confidence interval, and a p-value of less than 0.05 indicated a statistically significant difference.

3. Results

3.1. Bacterial decontamination

The application of the 810 nm diode laser resulted in a statistically significant reduction in *S. aureus* concentration across all intervention groups compared to the positive control ($p < 0.05$) (Figure 2). The average bacterial concentration in the positive control group was $8.6 \times 10^5 \pm 2 \times 10^5$ CFU/mL. Following laser irradiation, the residual bacterial concentrations were measured at $5.5 \times 10^5 \pm 9.4 \times 10^4$ CFU/mL for the 1 W group, $3.5 \times 10^5 \pm 5.8 \times 10^4$ CFU/mL for the 1.5 W group, $2.5 \times 10^5 \pm 5.8 \times 10^4$ CFU/mL for the 2 W group, and $2 \times 10^5 \pm 3.4 \times 10^4$ CFU/mL for the 2.5 W group.

The decontamination efficiency demonstrated a dose-dependent trend, with percentage reductions of 35.5%, 59.5%, 71.2%, and 76.6% corresponding to power levels of 1 W, 1.5 W, 2 W, and 2.5 W, respectively. While pairwise comparisons showed significant improvements in bacterial reduction as power increased from 1 W to 2 W ($p < 0.05$), the difference in effectiveness between the 2 W and 2.5 W groups was not statistically significant ($p = 0.191$).

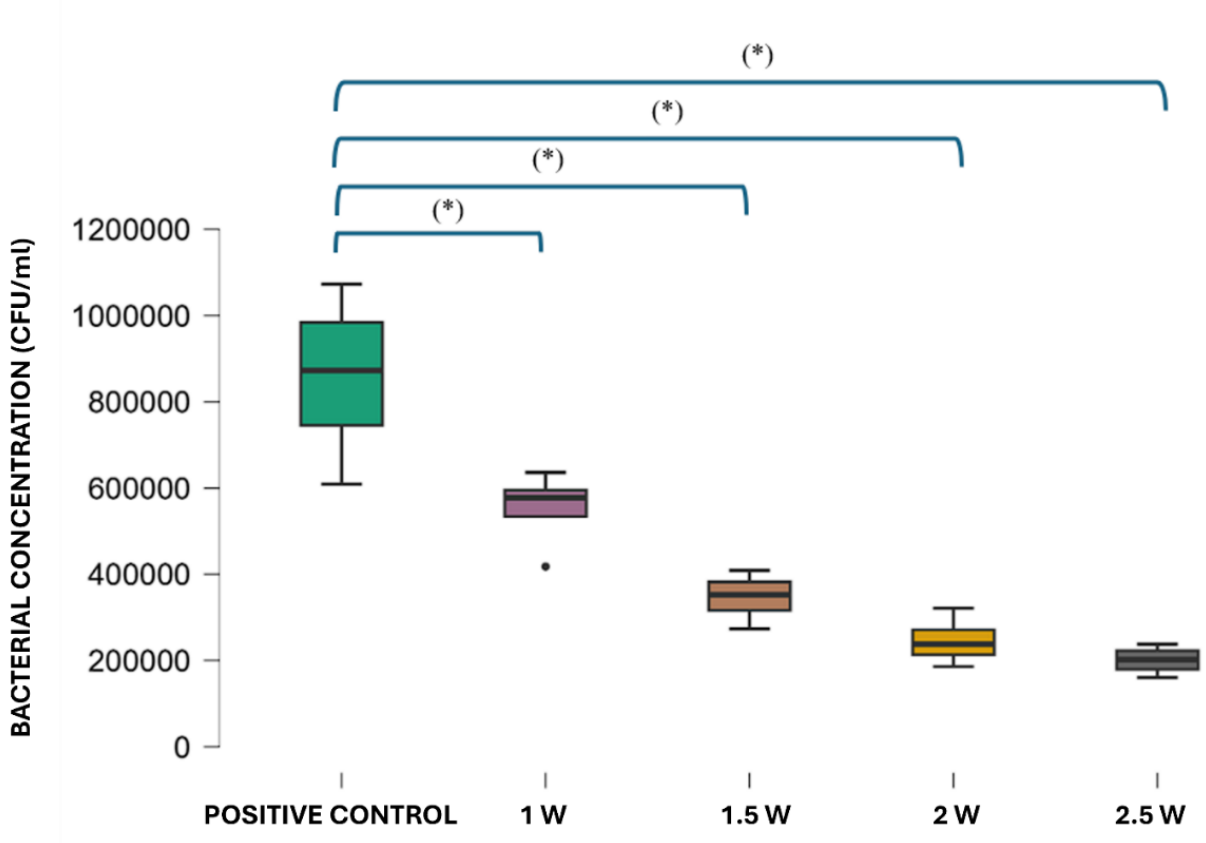

Figure 2. Comparison of average bacterial concentration across experimental groups. * indicates the Mann-Whitney U test ($p < 0.05$).

3.2. Surface roughness

The quantitative analysis of surface topography indicated that the Ra of the titanium implants was affected differently by varying laser power levels (Table 1). The baseline Ra values for the negative control and positive control were statistically similar, confirming that the initial bacterial contamination process did not alter the Ra. Following decontamination at lower power settings of 1 W and 1.5 W, the Ra values showed a slight downward trend compared to the controls, but the differences were not statistically significant ($p > 0.05$).

In contrast, irradiation at higher power levels led to an increase in Ra. While the Ra for the 2 W group did not reach statistical significance when compared to the control groups ($p = 0.19$), at the 2.5 W power level, the Ra showed a statistically significant increase compared to the positive control group ($p = 0.04$). Furthermore, a pairwise comparison revealed that the Ra at 2.5 W was significantly higher than that of the 1 W group ($p = 0.027$).

Table 1. Comparison of average surface roughness (Ra) across experimental groups.

Group	Mean Ra ± SD (μm)	Median (Range) (μm)	P-value (vs Positive Control)
Negative Control (n = 5)	0.85 ± 0.63	0.63 (0.07–3.25)	-
Positive Control (n = 5)	0.82 ± 0.57	0.54 (0.07–3.35)	-
1 W Laser (n = 20)	0.76 ± 0.51	0.49 (0.16–3.14)	0.91
1.5 W Laser (n = 20)	0.81 ± 0.45	0.52 (0.16–3.29)	0.82
2 W Laser (n = 20)	1.02 ± 0.64	0,72 (0.24–5.46)	0.19
2.5 W Laser (n = 20)	0.92 ± 0.49	0,69 (0.31–1.75)	0.04(*)

* Mann-Whitney U test ($p < 0.05$).

3.3. Surface morphology

SEM examination provided a detailed qualitative overview of the micro-structural changes induced by laser irradiation (Figure 3).

- Positive control Group: Implants exhibited a typical SLA micro-porous structure characterized by irregular pits, sharp edges, and clearly defined ridges.
- 1 W Group: The surface morphology remained largely unchanged even at X5000 magnification, retaining its characteristic sharp features and micro-porosity.
- 1.5 W Group: Observations at X5000 magnification revealed a slight reduction in the sharpness of the edges and ridges, although the primary micro-porous structure was preserved.
- 2 W Group: Significant morphological alterations were noted, including a loss of edge sharpness and a reduction in the size of the micro-pores. Additionally, small fragments of titanium debris were observed separating from the surface, particularly in the middle thread area.
- 2.5 W Group: The most severe damage occurred at this power level. The micro-pores appeared narrowed, sharp features were replaced by blunted topography, and there was a marked increase in titanium debris and surface scratches.

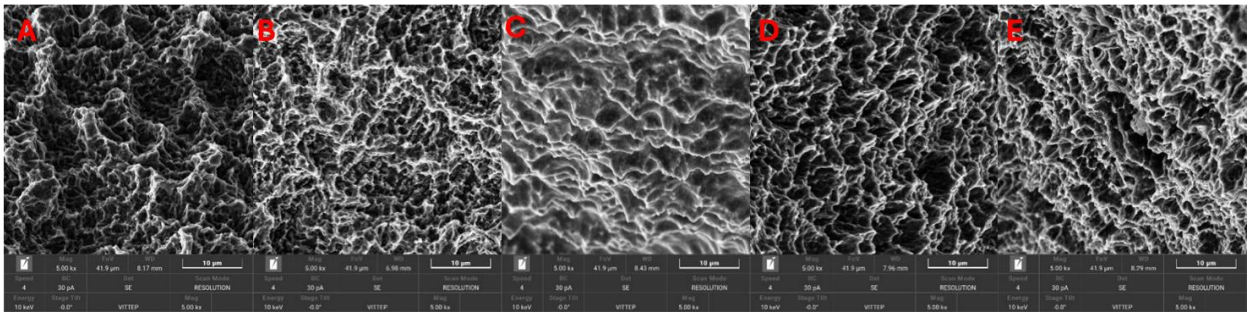

Figure 3. SEM micrographs (X5000) evaluating the impact of 810 nm diode laser power on the SLA surface of dental implants. (A) Positive control; (B) 1 W; (C) 1.5 W; (D) 2 W; and (E) 2.5 W irradiation groups.

4. Discussion

4.1. Bacterial decontamination

The results demonstrated a clear dose-dependent antimicrobial effect, with bacterial reductions ranging from 35.5% at 1 W to 76.6% at 2.5 W. While higher power levels significantly enhanced decontamination, the lack of statistical difference between the 2 W and 2.5 W groups suggests a plateau in efficacy at higher energy densities within the 3-minute exposure window.

When comparing our results to the literature, a significant discrepancy in reduction percentages emerges. Giannelli et al. [27] and Kreisler et al. [28] reported bacterial reductions exceeding 99% using similar 810 nm wavelengths. However, these researchers primarily utilized flat titanium discs. Our lower reduction rates (max 76.6%) are likely due to the use of real dental implants with intricate thread designs. These threads create "shadow zones" and recessed areas (troughs) where bacteria are shielded from direct laser irradiation. This is further supported by another study [18], which entailed actual implants and revealed that while some species like *Porphyromonas gingivalis* were eliminated, others like *Enterococcus faecalis* showed only a 50% reduction at 2.5 W, highlighting species-specific sensitivity and the impact of implant macro-morphology.

It is worth noting that the maximum bacterial reduction of 76.6% achieved at 2.5 W in this study equates to less than a 1-log microbial reduction. In classical microbiology, standard disinfection or sterilization typically requires a 3-log (99.9%) reduction or higher to be considered effective as a standalone treatment. However, in clinical practice, laser therapy is rarely utilized as a monotherapy in peri-implantitis treatment. It is critical to clarify that while the laser protocol was evaluated as an isolated, standalone intervention within this in vitro laboratory design to prevent confounding variables, it is strictly intended as an adjunctive modality within a comprehensive clinical peri-implantitis regimen. International guidelines have stated that laser therapy should be positioned as an adjunctive tool rather than a standalone treatment [9,29]. In a comprehensive peri-implantitis treatment regimen, conventional mechanical debridement using titanium brushes or ultrasonic scalers must first be employed to remove bulk calculus and thick biofilm layers. The laser protocol should then be implemented as a non-contact biophysical disinfectant. In addition, the true clinical value of the 810 nm diode laser lies not only in monotherapy, but also in its ability to physically and thermally disrupt the extracellular polymeric substance matrix of the biofilm. This structural disruption compromises

the biofilm's integrity, thereby increasing the susceptibility of the remaining bacterial cells to the host's immune response and to concurrent antimicrobial agents.

4.2. Topographical integrity

A major concern in laser-assisted decontamination is the preservation of the SLA (Sandblasted, Large-grit, Acid-etched) surface, which is essential for osteoblast attachment. Our quantitative analysis showed that the Ra remained statistically stable up to 2 W compared to the positive control. However, at 2.5 W, Ra significantly increased, indicating a threshold where thermal energy begins to physically alter the titanium.

SEM examination at X5000 magnification provided a deeper insight into this damage. While the 1 W group was indistinguishable from the control, the 2 W and 2.5 W groups exhibited ridges and ridges blunting, titanium debris, and pore narrowing.

In contrast, Faramarzi et al. [26] found no significant Ra changes at 2.5 W and 3.5 W using an 810 nm laser. The difference lies in the exposure time; the author's protocol involved only 10 seconds of irradiation per site, whereas we applied 1 minute per section. This confirms that the cumulative thermal load, a product of power and duration, is the primary driver of surface degradation. The appearance of surface scratches and narrowed pores at 2.5 W in our study serves as a definitive marker for the upper safety limit of continuous-wave 810 nm diode lasers on SLA surfaces.

In this study, the Ra values for the 2 W group exhibited no statistically significant difference when compared to the positive; yet, high-magnification SEM examinations at this identical power level revealed localized micro-structural degradation, including a loss of edge sharpness and the separation of titanium debris. This discrepancy confirms that the 2D Ra metric is too insensitive to isolate localized "hot spots" of thermal degradation induced by continuous-wave laser application. Because Ra is an arithmetic line average calculated along a single linear track, extreme localized deviations confined to narrow zones, such as the thread troughs where thermal energy accumulates, are mathematically diluted and flattened. Despite this limitation, Ra is the most widely recognized and standardized metric in dental materials research. Utilizing it enables a direct, reliable baseline comparison between our data and the vast majority of historical implant manufacturing literature. In future investigations, researchers should transition to 3D optical profiling, utilizing areal roughness parameters to accurately capture localized micro-structural modifications and validate surface biocompatibility before clinical translation.

4.3. Strengths, limitations, and research outlook

A primary strength of this study is the high level of clinical relevance achieved through the use of actual dental implants featuring intricate thread designs and a standardized SLA surface treatment. Unlike many researchers who have utilized flat titanium discs, our model more accurately simulates the "shadow zones" and recessed topographical features where biofilms accumulate in a clinical setting. Furthermore, we employed a custom-designed mechanical holder and stand system, which ensured a constant distance and perpendicular orientation between the laser tip and the implant surface. By utilizing a surgical motor to maintain a consistent rotation speed of 20 rpm and a sliding track for precise parallel movement, the experimental setup eliminated the operator-dependent variability inherent in manual laser handling, thereby ensuring a high degree of standardization and repeatability

across all intervention groups. This enabled a highly controlled evaluation of how increasing power densities influence bacterial reduction and surface integrity.

Despite the standardized experimental design, several limitations must be acknowledged, primarily related to the in vitro nature of the research. We utilized a single-species biofilm model (*S. aureus*) over a 72-hour incubation period, which does not fully represent the complex, multi-species anaerobic communities and mature extracellular polymeric substances typically found in chronic clinical peri-implantitis. Additionally, the laboratory environment excluded the presence of biological fluids, such as saliva, blood, and gingival crevicular fluid, which can act as light absorbers or coolants during laser irradiation, potentially altering the energy absorption characteristics observed in this study. Clinical accessibility remains another significant factor; while the custom holder enabled an ideal perpendicular laser orientation, anatomical constraints in the oral cavity, such as bone morphology and soft tissue, often limited the angle and proximity of the laser tip during actual treatment. Consequently, clinical decontamination efficacy is expected to decrease due to an increase in unexposed thread surface area. This limitation reinforces that laser therapy cannot be used as a standalone monotherapy.

We utilized an 810 nm diode laser in continuous-wave (CW). This modality was selected because, according to the literature, continuous energy delivery provides a significantly higher antibacterial effect compared to pulsed modes at equivalent power levels. The uninterrupted photothermal exposure prevents intermediate bacterial recovery and more effectively denatures the biofilm matrix. However, the visible micro-structural alterations observed at 2.5 W, such as the blunting of structural ridges, narrowing of micro-pores, and shedding of titanium debris, demonstrate the impact of the cumulative thermal load associated with CW emission over the 3-minute exposure window. Utilizing pulsed or gated delivery modes introduces a critical biophysical parameter known as thermal relaxation time [29–31]. This interval enables localized heat to dissipate from the titanium body between active laser peaks.

Furthermore, we did not incorporate real-time thermal monitoring during the irradiation process. Exceeding a local temperature of 47 °C for more than one minute at the alveolar bone interface is well-documented to induce irreversible osteonecrosis, micro-vascular collapse, and subsequent implant failure [32]. Although topographical changes were assessed via SEM and profilometry, the lack of temperature data means the potential for heat conduction to the surrounding alveolar bone remains unquantified, which is a critical safety threshold for clinical application.

In future studies, researchers should prioritize multi-species biofilm models and incorporate thermal sensors to map the safety profile of the 810 nm laser regarding bone-to-implant contact temperatures. Additionally, future protocols must entail pulsed or gated laser delivery modes rather than continuous-wave configurations. This will enable the optimization of thermal relaxation times, effectively mitigating heat accumulation at the bone-to-implant interface while maintaining predictable biofilm eradication.

5. Conclusions

The 810 nm diode laser effectively reduces *S. aureus* on SLA implants in a dose-dependent manner. While decontamination peaked with 2.5 W, this power level significantly compromised surface roughness and micro-morphology. In contrast, power levels up to 2 W successfully preserved the implant's micro-morphology and structural integrity. Balancing microbial reduction with surface preservation, 2 W in continuous mode appears to be suitable for implant decontamination in vitro.

Because this study was performed under the standardized conditions of an in vitro laboratory, these outcomes cannot be interpreted as general clinical efficacy parameters for active peri-implantitis treatment. Further validation via real-time bone-bed thermal mapping is required before definitive clinical safety thresholds can be established.

Use of AI tools declaration

The authors declare they have not used Artificial Intelligence (AI) tools in the creation of this article.

Conflict of interest

The authors declare no conflict of interest.

Author contributions

Conceptualization: Thuy Vo, Loan Pham; Data curation: Luong Dau, Cao Duc; Formal analysis: Cao Duc, Bui Lam; Investigation: Thuy Vo, Tien Ho; Methodology: Thuy Vo, Loan Pham, Bui Lam; Project administration: Loan Pham; Visualization: Thuy Vo, Bui Lam; Writing–original draft: Thuy Vo; Writing–review editing: Loan Pham, Tien Ho

References

1. French D, Ofec R, Levin L (2021) Long term clinical performance of 10 871 dental implants with up to 22 years of follow-up: a cohort study in 4247 patients. *Clin Implant Dent Relat Res* 23: 289–297. https://doi.org/10.1111/cid.12994
2. Rakic M, Galindo-Moreno P, Monje A, et al. (2018) How frequent does peri-implantitis occur? A systematic review and meta-analysis. *Clin Oral Investig* 22: 1805–1816. https://doi.org/10.1007/s00784-017-2276-y
3. Ting M, Craig J, Balkin BE, et al. (2018) Peri-implantitis: a comprehensive overview of systematic reviews. *J Oral Implantol* 44: 225–247. https://doi.org/10.1563/aaid-joi-D-16-00122
4. Kadirvelu L, Sivaramalingam SS, Jothivel D, et al. (2024) A review on antimicrobial strategies in mitigating biofilm-associated infections on medical implants. *Curr Res Microb Sci* 6: 100231. https://doi.org/10.1016/j.crmicr.2024.100231
5. Quirynen M, Vogels R, Peeters W, et al. (2006) Dynamics of initial subgingival colonization of 'pristine' peri-implant pockets. *Clin Oral Implants Res* 17: 25–37. https://doi.org/10.1111/j.1600-0501.2005.01194.x
6. Furst MM, Salvi GE, Lang NP, et al. (2007) Bacterial colonization immediately after installation on oral titanium implants. *Clin Oral Implants Res* 18: 501–508. https://doi.org/10.1111/j.1600-0501.2007.01381.x
7. Kronström M SB, Erickson E, Houston L, et al. (2000) Humoral immunity host factors in subjects with failing or successful titanium dental implants. *J Clin Periodontol* 27: 875–882. https://doi.org/10.1034/j.1600-051x.2000.027012875.x

8. Persson GR and Renvert S (2014) Cluster of bacteria associated with peri-implantitis. *Clin Implant Dent Relat Res* 16: 783–793. https://doi.org/10.1111/cid.12052
9. Roccuzzo A, Stähli A, Monje A, et al. (2021) Peri-implantitis: a clinical update on prevalence and surgical treatment outcomes. *J Clin Med* 10: 1107. https://doi.org/10.3390/jcm10051107
10. Herrera D, Berglundh T, Schwarz F, et al. (2023) Prevention and treatment of peri-implant diseases-The EFP S3 level clinical practice guideline. *J Clin Periodontol* 50: 4–76. https://doi.org/10.1111/jcpe.13823
11. Baima G, Citterio F, Romandini M, et al. (2022) Surface decontamination protocols for surgical treatment of peri-implantitis: a systematic review with meta-analysis. *Clin Oral Implants Res* 33: 1069–1086. https://doi.org/10.1111/clr.13992
12. Mellado-Valero A, Buitrago-Vera P, Sola-Ruiz MF, et al. (2013) Decontamination of dental implant surface in peri-implantitis treatment: a literature review. *Med Oral Patol Oral Cir Bucal* 18: e869–e876. https://doi.org/10.4317/medoral.19420
13. Marotti J, Tortamano P, Cai S, et al. (2013) Decontamination of dental implant surfaces by means of photodynamic therapy. *Lasers Med Sci* 28: 303–309. https://doi.org/10.1007/s10103-012-1148-6
14. Valente NA, Mang T, Hatton M, et al. (2017) Effects of two diode lasers with and without photosensitization on contaminated implant surfaces: an ex vivo study. *Photomed Laser Surg* 35: 347–356. https://doi.org/10.1089/pho.2016.4247
15. Romanos GE, Gutknecht N, Dieter S, et al. (2009) Laser wavelengths and oral implantology. *Lasers Med Sci* 24: 961–970. https://doi.org/10.1007/s10103-009-0676-1
16. Ting M, Alluri LSC, Sulewski JG, et al. (2022) Laser treatment of peri-implantitis: a systematic review of radiographic outcomes. *Dent J* 10: 20. https://doi.org/10.3390/dj10020020
17. Tosun E, Tasar F, Strauss R, et al. (2012) Comparative evaluation of antimicrobial effects of Er:YAG, diode, and CO_2 lasers on titanium discs: an experimental study. *J Oral Maxillofac Surg* 70: 1064–1069. https://doi.org/10.1016/j.joms.2011.11.021
18. Gonçalves F, Zanetti A L, Zanetti R V, et al. (2010) Effectiveness of 980-mm diode and 1064-nm extra-long-pulse neodymium-doped yttrium aluminum garnet lasers in implant disinfection. *Photomed Laser Surg* 28: 273–280. https://doi.org/10.1089/pho.2009.2496
19. Azma E and Safavi N (2013) Diode laser application in soft tissue oral surgery. *J Lasers Med Sci* 4: 206–211.
20. Ortega-Concepción D, Cano-Durán JA, Peña-Cardelles JF, et al. (2017) The application of diode laser in the treatment of oral soft tissues lesions. A literature review. *J Clin Exp Dent* 9: e925–e928. https://doi.org/10.4317/jced.53795
21. Roncati M, Lucchese A, Carinci F (2013) Non-surgical treatment of peri-implantitis with the adjunctive use of an 810-nm diode laser. *J Indian Soc Periodontol* 17: 812–815. https://doi.org/10.4103/0972-124X.124531
22. Saffarpour A, Nozari A, Fekrazad R, et al. (2018) Microstructural evaluation of contaminated implant surface treated by laser, photodynamic therapy, and chlorhexidine 2 percent. *Int J Oral Maxillofac Implants* 33: 1019–1026. https://doi.org/10.11607/jomi.6325
23. Kushima SS, Nagasawa M, Shibli JA, et al. (2016) Evaluation of temperature and roughness alteration of diode laser irradiation of zirconia and titanium for peri-implantitis treatment. *Photomed Laser Surg* 34: 194–199. https://doi.org/10.1089/pho.2015.4026

24. Castro GL, Gallas M, Nunez IR, et al. (2007) Scanning electron microscopic analysis of diode laser-treated titanium implant surfaces. *Photomed Laser Surg* 25: 124–128. https://doi.org/10.1089/pho.2006.1086
25. Monzavi A, Fekrazad R, Chinipardaz Z, et al. (2018) Effect of Various Laser Wavelengths on Temperature Changes During Periimplantitis Treatment: an in vitro study. *Implant Dent* 27: 311–316. https://doi.org/10.1097/ID.0000000000000751
26. Faramarzi M, Sadighi M, Mirhashemi S (2018) Evaluation of surface changes of dental implants after irradiation with diode laser beams with different energies: a sem study. *J Adv Periodontol Implant Dent* 10: 85–89. https://doi.org/10.15171/japid.2018.013
27. Giannelli M, Landini G, Materassi F, et al. (2016) The effects of diode laser on Staphylococcus aureus biofilm and Escherichia coli lipopolysaccharide adherent to titanium oxide surface of dental implants. An in vitro study. *Lasers Med Sci* 31: 1613–1619. https://doi.org/10.1007/s10103-016-2025-5
28. Kreisler M, Kohnen W, Marinello C, et al. (2003) Antimicrobial efficacy of semiconductor laser irradiation on implant surfaces. *Int J Oral Maxillofac Implants* 18: 706–711.
29. Deppe H, Ahrens M, Behr AV, et al. (2021) Thermal effect of a 445 nm diode laser on five dental implant systems: an in vitro study. *Sci Rep* 11: 20174. https://doi.org/10.1038/s41598-021-99709-8
30. Giannelli M, Lasagni M, Bani D (2015) Thermal effects of lambda = 808 nm GaAlAs diode laser irradiation on different titanium surfaces. *Lasers Med Sci* 30: 2341–2352. https://doi.org/10.1007/s10103-015-1801-y
31. Geminiani A, Caton JG, Romanos GE (2012) Temperature change during non-contact diode laser irradiation of implant surfaces. *Lasers Med Sci* 27: 339–342. https://doi.org/10.1007/s10103-010-0876-8
32. Eriksson RA and Albrektsson T (1984) The effect of heat on bone regeneration: an experimental study in the rabbit using the bone growth chamber. *J Oral Maxillofac Surg* 42: 705–711. https://doi.org/10.1016/0278-2391(84)90417-8